Journal of Materials Chemistry B

Accepted Manuscript

ROYAL SOCIETY OF CHEMISTRY

www.rsc.org/materialsB

Journal of Materials Chemistry B RSCPublishing

PAPER

Influence of reduction-sensitive diselenide bonds and disulfide bonds on oligoethylenimine conjugates for gene delivery

Cite this: DOI: 10.1039/x0xx00000x

Received 00th January 2013,
Accepted 00th January 2013

DOI: 10.1039/x0xx00000x

www.rsc.org/

Dong Yue, Gang Cheng, Yiyan He, Yu Nie, Qian Jiang, Xiaojun Cai* and Zhongwei Gu*

Bioreducible polymers have appeared as ideal gene delivery vectors due to the high stability in extracellular fluids and rapid DNA unpacking in intracellular reducing environment, as well as decreased cytotoxicity. Disulfide bonds have long been regarded as the only golden standard for this design. Recently, diselenide bonds have emerged as a new reduction-sensitive linkage. However, its reduction sensitivity has not been systemically reported. The primary aim of this study is to compare its reduction sensitivity with the golden standard disulfide bonds. Bioreduction-triggered polymers degradation revealed that diselenide bonds are more stable than disulfide bonds with a lower redox potential (i.e. 10 μM GSH). The changes in DNA binding ability, particle size, zeta potential, and morphology all demonstrated that diselenide bonds have similar reduction sensitivity as disulfide bonds, but it could be only cleaved at a tumor-relevant glutathione concentration (i.e. 10 mM GSH). Förster resonance energy transfer (FRET) spectra suggested that diselenide bonds conjugated OEI800 (OEI-$SeSe_x$) complexes could not only maintain high stability in 10 μM GSH conditions, but also timely release DNA in 10 mM GSH conditions. Cell viability assay results showed OEI-$SeSe_x$ has similar cell viability profile as disulfide bond conjugated OEI800 (OEI-SS_x), which is much lower toxic than PEI25k. Biological efficacy assessment indicated comparable or even outweigh transfection efficiency of OEI-$SeSe_x$ with OEI-SS_x and PEI25k. These results suggested that the unique properties of diselenide bonds have enabled versatile design of multifunctional bioreducible polymers for *in vivo* gene delivery.

Introduction

Gene therapy provides a promising paradigm for the treatment of various acquired or congenital diseases, such as cystic fibrosis, severe combined immunodeficiency, diabetes, cancer and infectious diseases.[1-4] In gene therapy, genetic materials, either RNA or DNA, are transferred into specific human tissues or cells to replace defective genes, substitute missing genes, silence unwanted gene expression or introduce new cellular biofunctions.[5,6] Thus, the key challenge in realizing the full potential of gene therapy is the development of efficient yet safety delivery vehicles that are capable of mediating high and sustained levels of gene expression.[7-9] Viral vectors are evidently most effective, but pose safety issues such as healthy cell infection, inflammation, immunogenicity, carcinogenicity and the possibility of gene recombination.[10-12] Alternatively, non-viral gene delivery vectors are receiving a tremendous amount of interest due to their limited immunogenicity, respectable DNA loading capacity, easy of preparation and versatility for chemical modification.[13-16]

Most non-viral vectors are made of cationic lipids and polymers. Among them, branched polyethylenimine (PEI) has been shown to be one of the most efficient synthetic gene delivery vectors *in vitro* and has been widely used as the benchmark polymer vector.[17,18] PEI condenses DNA to nano-sized complexes for easier endocytosis. Once in the cells, the proton sponge effect, buffering and membrane lytic capacity of PEI can benefit the endosomal escape of complexes. However, transfection efficiency and cytotoxicity of PEI depends on the molecular weight and it is generally accepted that PEI with a higher molecular weight (i.e. 25 kDa) shows high transfection efficiency and cytotoxicity.[19,20] In contrast, low molecular weight PEI has low cytotoxicity but cannot effectively condense DNA and has poor transfection efficiency.[21] Therefore, a viable strategy is to design biodegradable PEI which can allow efficient gene transfer and stimulus-responsive

degradation into low molecular weight products with minimal toxicity.

It has been well documented that intracellular and extracellular environments differ in pH,[22,23] enzymatic activity [24,25] and redox potential.[26-28] These factors can be used as triggers for disassociation of polyplexes. Intracellular glutathione levels (approximately 2-10 mM) are 2 to 3 orders higher than that of in extracellular fluids (approximately 2-20 μM).[27,29] Therefore, disulfide bonds have been widely used for reductive design in gene and drug delivery. The dynamic chemical stability of disulfide bonds, i.e. superior stability under the extracellular environment and rapid degradation in the intracellular reducing conditions, could elegantly resolve the contradictory requirements of efficient non-viral gene transfer agents, i.e. excellent binding and protection of nucleic acids in extracellular fluids and efficient release of nucleic acids inside the cells.[27] Owing to these unique features, vast disulfide bond conjugated PEIs have been developed for intracellular gene delivery.[30-32] In addition to bringing about enhanced transfection efficiency, these carriers also show largely improved toxicity profiles due to the decreased charge density upon intracellular cleavage of disulfide bonds.

Inspired by the success of disulfide bonds, the selenium (Se) element listed in the same family as sulfur (S) in the periodic table of elements has attracted attention. Since selenium and sulfur are similar in many respects, including electronegativity, atom size and accessible oxidation states,[28] diselenide bonds are hypothesized having similar reduction sensitivity as disulfide bonds. Zhang et al. reported that micelles formed by the polymers containing diselenide bonds were quite stable under physiological conditions, but were sensitive to reductive stimuli.[33] Similar results were also recently reported from our studies that cross-linked oligoethylenimine (OEI800) using diselenide bonds have gained encouraging transfection efficiency together with minimal toxicity.[34] However, few studies have focused on comparing its reduction sensitivity with the golden standard disulfide bonds, as well as its influence on polyplexes transfection.

In this study, two kinds of bioreducible cationers, diselenide bonds conjugated OEI800 (OEI-SeSe$_x$) and disulfide bonds conjugated OEI800 (OEI-SS$_x$) were developed for comparison of the reduction sensitivity between diselenide bonds and disulfide bonds. Their redox-sensitivity was tested and compared by monitoring polymer degradation, particle size and zeta potential alterations, DNA binding ability changes and DNA unpacking kinetics. Its influence on gene expression was also evaluated *in vitro* using the pGL3 and pEGFP as the reporter genes in 4T1, B16F10 and HeLa cells.

Results and discussion

Synthesis of OEI-SeSe$_x$ and OEI-SS$_x$

The synthetic route of diselenide conjugated OEI800 (OEI-SeSe$_x$) and disulfide conjugated OEI800 (OEI-SS$_x$) was shown in Fig. 1. Briefly, the diselenide bonds containing linker DSeDPA was first synthesized, then the carboxyl group at the terminal end of DSeDPA and DSDPA was activated by NHS, using EDC as the dehydrolyzing agent in THF to obtain active ester. The active ester reacted with the primary amine group of OEI800, resulting in the diselenide bonds conjugated OEI800 (OEI-SeSe$_x$) and disulfide bonds conjugated OEI800(OEI-SS$_x$), respectively. It should be noted that at the cross-linking step, the concentration of OEI800 must be controlled, which was

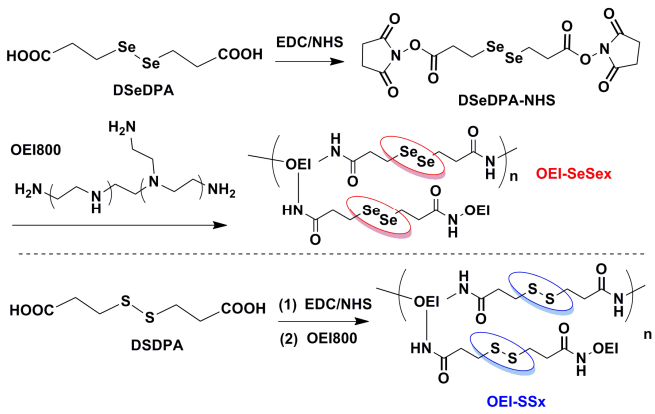

Fig.1 Synthetic schema for diselenide bonds conjugated oligoethylenimine (OEI-SeSe$_x$) and disulfide bonds conjugated oligoethylenimine (OEI-SS$_x$).

significantly related to the molecular weight of the final products. Higher molecular weight of the cross-linked products would be obtained, because the intermolecular reaction occurs easily at higher OEI800 concentrations.[35] For example, OEI-SeSe$_x$ and OEI-SS$_x$ with *M*w of 18 kDa and 17 kDa, respectively, was obtained at OEI800 concentration of 25%. Whereas, OEI-SeSe$_x$ with *M*w of 11.5 kDa and 7 kDa was obtained at OEI800 concentration of 15% and 10%, respectively. These bioreducible cationers were designated as OEI-SeSe$_x$(18k), OEI-SS$_x$(17k), OEI-SeSe$_x$(11.5k) and OEI-SeSe$_x$(7k), respectively. Besides, it is noteworthy that PEI25k has the similar *M*w with OEI-SeSe$_x$(18k) and OEI-SS$_x$(17k) under the same GPC test conditions, their *M*w are 20, 18 and 17 kDa, respectively (Table 1). Therefore, PEI25k was served as a positive control to evaluate the cell viability and transfection efficiency of OEI-SeSe$_x$ and OEI-SS$_x$.

	Molecular weights		
polymers	$M_w/10^3$	$M_n/10^3$	PDI
OEI-SeSe$_x$(18k)	18	5.3	3.4
OEI-SeSe$_x$(11.5k)	11.5	3.6	3.2
OEI-SeSe$_x$(7k)	7	2.3	3.0
OEI-SS$_x$(17k)	17	4.9	3.5
PEI25k	20	7.8	2.6
OEI800	0.7	0.5	1.5

Table 1 Molecular weights of various polymers detected by gel permeation chromatograph.
Abbreviations: *M*w, weight-average molecular weight; *M*n, number-average molecular weight; PDI, polydispersity index.

Bioreduction-triggered polymer degradation

For comparison the reduction sensitivity between diselenide bonds and disulfide bonds, bioreducible cationers OEI-SeSe$_x$ and OEI-SS$_x$ were treated with gradient GSH levels (i.e. 10 μM and 10 mM GSH mimicking the extracellular and intracellular GSH levels, respectively) at 37 °C for 4 h or 8 h, respectively. Time-dependent changes in molecular weight and molecular weight distribution of different cationers were monitored by

GPC. As shown in Fig. 2, the peak shift of OEI-$SeSe_x$ and OEI-SS_x in GPC became diversified. The peaks of OEI-SS_x(17k) (Fig. 2B) obviously shifted to a longer point after treatment with 10 μM GSH for 8 h, indicating a significant decrease in molecular weight due to the redox-induced cleavage of disulfide bonds, while that of OEI-$SeSe_x$(18k) (Fig. 2A), OEI-$SeSe_x$(11.5k) (Fig. S1) and OEI-$SeSe_x$(7k) (Fig. S1) remained constant under identical conditions. When incubated with a thousand-fold concentration of GSH of 10 mM for 2 h, both OEI-$SeSe_x$(18k) and OEI-SS_x(17k) degraded. These results demonstrated that diselenide bonds have similar reduction sensitivity as disulfide bonds, but are stable than disulfide bonds with a lower redox-potential.

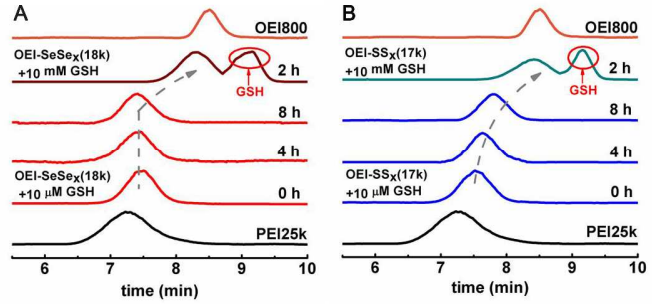

Fig.2 GPC diagrams of bio-reducible polymers before and after degradation in response to redox stimuli (10 μM GSH) for 4 h or 8 h, and (10 mM GSH) for 2 h, OEI-$SeSe_x$(18k) (A), OEI-SS_x(17k) (B).

DNA binding ability with or without reduction reagents

The ability of catiomer to condense DNA into stable complexes is a prerequisite to protect DNA from being digested by enzymes and endosome acidic conditions.[36] Here, agarose gel retardation assay was performed to evaluate the DNA binding ability of OEI-$SeSe_x$ and OEI-SS_x. As shown in Fig. 3, high molecular weight catiomers, including OEI-$SeSe_x$(18k) (Fig. 3A1), OEI-SS_x(17k) (Fig. 3B1) and PEI25k (Fig. 3C) could efficiently retard DNA migration at a catiomer/pDNA weight ratio of 0.5, 0.5 and 0.3, respectively, while OEI800 showed no DNA binding ability even at c/p ratio up to 0.8 (Fig. 3D). These results suggested that the DNA binding ability of catiomers increases with increasing molecular weight of catiomers.

After treatment with GSH, the ability of OEI-SS_x(17k) and OEI-$SeSe_x$(18k) to complex with DNA became diversified. For instance, incubation for 30 min in the presence of 10 μM GSH allowed remarkable migration of negatively charged DNA toward the anode from OEI-SS_x(17k) complexes at a catiomer/pDNA weight ratio (c/p) of 0.7 (Fig. 3B2), while no detectable migrations were observed for OEI-$SeSe_x$(18k) complexes (Fig. 3A2). Combined with the results from the reduction sensitive-triggered polymer degradation kinetics (Fig. 2), it was concluded that the degradation of OEI-SS_x(17k) via the reductive cleavage of disulfide bonds in 10 μM GSH could account for the decreased DNA binding ability.

Furthermore, after a short-term exposure to 10 mM GSH, a visible DNA migration was also observed for OEI-$SeSe_x$(18k) complexes (Fig. 3A3), which implied the reduction sensitive ability for diselenide bonds, and its reductive cleavage could also facilitate the payload DNA release in the presence of tumor-relevant GSH concentrations. These results demonstrated that diselenide bonds have similar reduction sensitivity as disulfide bonds, but it could be only cleaved at a tumor-relevant GSH concentration, indicating diselenide bonds are more stable than disulfide bonds.

Biophysical characterization of catiomer/pDNA complexes with or without reduction reagents

Particle size distribution, surface charge and morphology of catiomer/pDNA complexes strongly influence cytotoxicity, cellular uptake/intracellular trafficking, and release of genetic payload.[37] Morphometric analysis of OEI-SS_x/pDNA or OEI-$SeSe_x$/pDNA complexes was performed by DLS and TEM, respectively.

As shown in Fig. 4A, all catiomers including PEI25k, OEI-SS_x(17k), OEI-$SeSe_x$(18k), OEI-$SeSe_x$(11.5k) and OEI-$SeSe_x$(7k) could condense pDNA into small complexes (c/p 1.3 for PEI25k, and c/p 6–10 for OEI-$SeSe_x$(18k), OEI-$SeSe_x$(11.5k) and OEI-$SeSe_x$(7k)), with diameters ranging from 126 to 304 nm, which was within the size requirements for efficient cellular endocytosis.[38] Whereas OEI800 forms the loosest polyplex with a size of about 1000 nm at a c/p ratio of 10 (data not shown). The sizes of the OEI-SS_x(17k) complexes remained

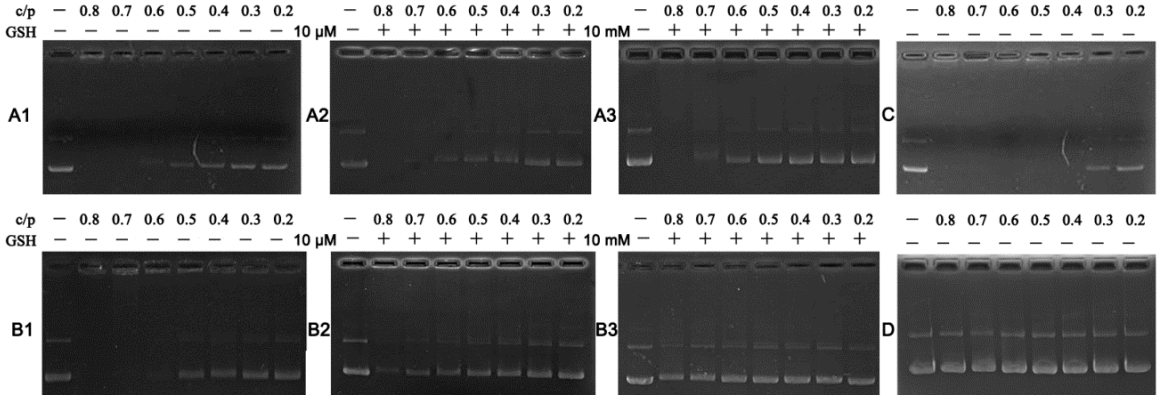

Fig.3 Gel retardation assay of various catiomers complexed with plasmid DNA (catiomer/pDNA weight ratio, c/p = 0.2-0.8). OEI-$SeSe_x$(18k) treated with 0 μM GSH (A1), 10 μM GSH (A2), 10 mM GSH (A3), OEI-SS_x(17k) treated with 0 μM GSH (B1), 10 μM GSH (B2), 10 mM GSH (B3), PEI25k treated with 0 μM GSH (C), OEI800 treated with 0 μM GSH (D).

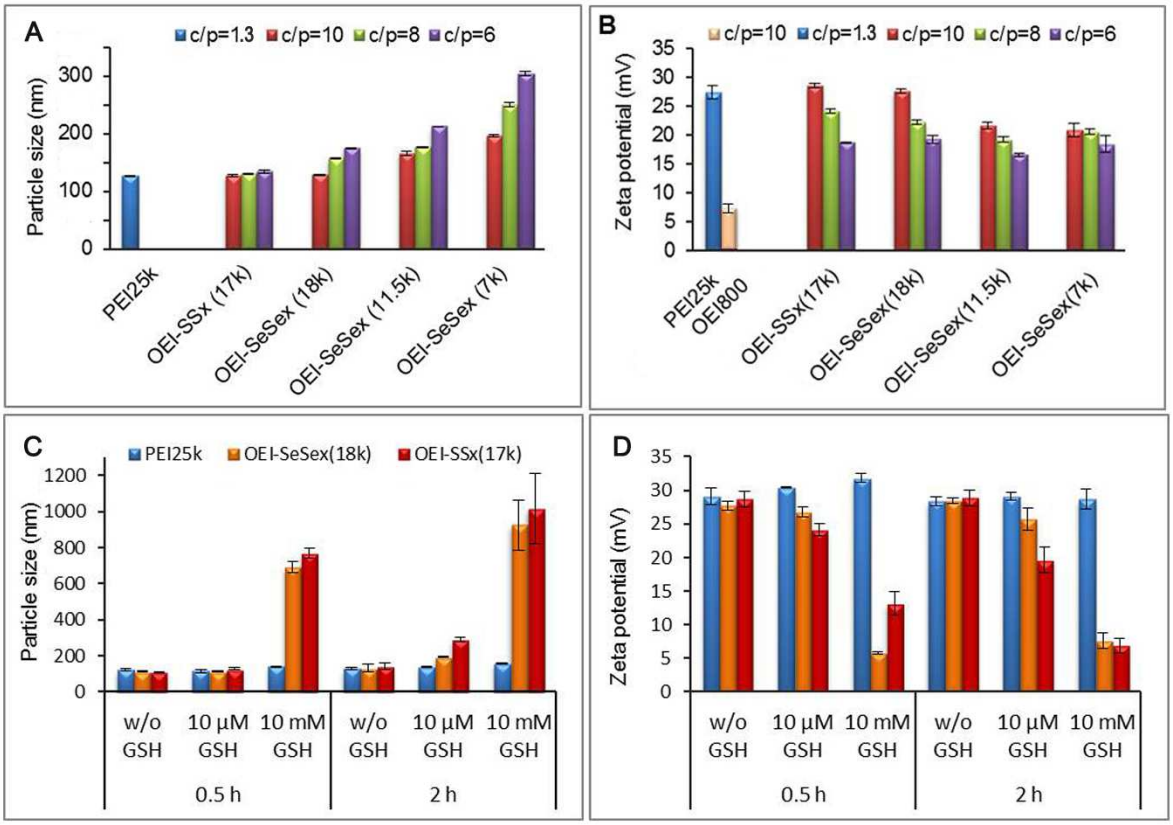

Fig.4 Particle size (A) and zeta potential (B) of various complexes composed of PEI25k, OEI-SS_x(17k), OEI-$SeSe_x$(18k), OEI-$SeSe_x$(11.5k), OEI-$SeSe_x$(7k) or OEI800 and DNA at different catiomer/pDNA weight ratios (c/p). Changes in particle size (C) and zeta potential (D) of OEI-$SeSe_x$(18k) and OEI-SS_x(17k) complexes (c/p = 8) in the absence or presence of 10 μM or 10 mM GSH at 37 °C for 30 min or 2 h, PEI25k complexes (c/p = 1.3) was served as control. Data are shown as mean ± SD (n = 3).

around at 130 nm at all tested catiomer/pDNA weight ratios (c/p) ranging from 6 to 10, which were similar to that of PEI25k complexes. The sizes of the OEI-$SeSe_x$ complexes tended to decrease with increasing c/p ratios. For instance, the sizes of OEI-$SeSe_x$(18k) complexes decreased from 175 nm to 130 nm, as the c/p ratio increased from 6 to 10. In addition, the sizes of OEI-$SeSe_x$ complexes tended to increase with decreasing molecular weight of catiomers, suggesting that high molecular weight OEI-$SeSe_x$ could bind and compact DNA more effectively. The zeta-potential of the well compacted catiomer/pDNA complexes increases with increasing c/p ratios (Fig. 4B). At a c/p ratio of 10, the mean surface charges of OEI-SS_x(17k) and OEI-$SeSe_x$(18k) complexes were 28 mV and 27 mV, respectively, similar to that of PEI25k complexes (27 mV), and the OEI800 polyplex has the lowest zeta potential of 7 mV.

After exposure to 10 μM GSH for 30 min, the particle size of OEI-$SeSe_x$(18k) complexes remained constant (113 nm) (Fig. 4C), while that of OEI-SS_x(17k) increased from 110 nm to 128 nm (Fig. 4C). It is noteworthy that OEI-$SeSe_x$(18k) complexes swelled gradually to 190 nm after 2 h incubation, while that of OEI-SS_x(17k) swelled rapidly to 290 nm. These results are consistent with the polymer degradation profiles shown in Fig. 2, implying OEI-$SeSe_x$(18k) are more stable than OEI-SS_x(17k) in 10 μM GSH conditions.

The continuous increase of concentration of GSH was hypothesized to lead to the complete dissociation of these complexes. As expected, after incubation with 10 mM GSH for 30 min, OEI-SS_x(17k) and OEI-$SeSe_x$(18k) complexes swelled rapidly to 770 nm and 690 nm, respectively, which even swelled to a final size about 1000 nm and 920 nm, respectively, after 2 h incubation. Besides, GSH treatment has no influence on the particle size of PEI25k/DNA complexes. The above phenomenon further demonstrated that diselenide bonds have similar reduction sensitivity as disulfide bonds, but are stable than disulfide bonds with a lower redox-potential.

Changes in zeta potential further strengthened this conclusion. For example, without GSH, the zeta potential of

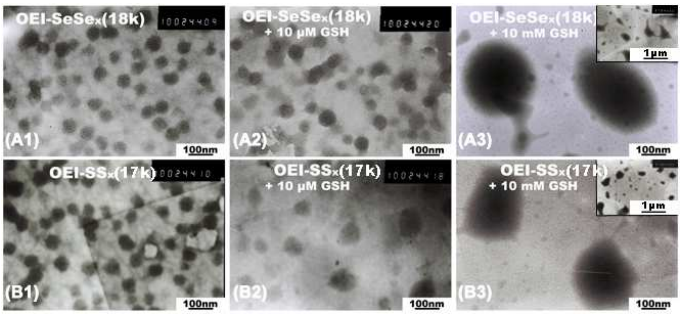

Fig.5 Typical TEM images of OEI-$SeSe_x$(18k) (A) and OEI-SS_x(17k) (B) complexes (c/p = 8) with or without (10 μM or 10 mM GSH) treatment. Bar = 100 nm or 1 μm.

OEI-SS_x(17k) and OEI-$SeSe_x$(18k) complexes was 28 mV and 27 mV (Fig. 4D), respectively. However, after incubation with 10 μM GSH for 30 min, the zeta potential of OEI-SS_x(17k) complexes decreased to 24 mV, while that of OEI-$SeSe_x$(18k) complexes remained constant (26.8 mV). Besides, the zeta potential of OEI-SS_x(17k) complexes gradually decreased to 19 mV after 2 h incubation, while that of OEI-$SeSe_x$(18k) complexes only decreased to 25 mV. On the other hand, treatment with 10 mM GSH for 2 h changed the zeta potential of OEI-SS_x(17k) and OEI-$SeSe_x$(18k) complexes sharply to 6 mV and 7 mV, respectively. We attribute the increased particle size and decreased zeta potential of OEI-SS_x and OEI-$SeSe_x$ complexes to redox-induced hydrolysis of disulfide bonds and diselenide bonds resulting in low molecular weight fragments, including OEI800 (Fig. 2), that are unable to efficiently condense DNA (Fig. 3D), thus resulting in the formation of much looser states of complexes with larger sizes around 1000 nm (Fig. 4C) and lower zeta potential around 7 mV (Fig. 4D), which is equal to the level of the OEI800 complexes about 1000 nm (data not shown) and 7 mV (Fig. 4B), and are consistent with the previous studies.[39]

The representative morphologies of OEI-SS_x(17k) and OEI-$SeSe_x$(18k) complexes at a c/p ratio of 8 are shown in Fig. 5.

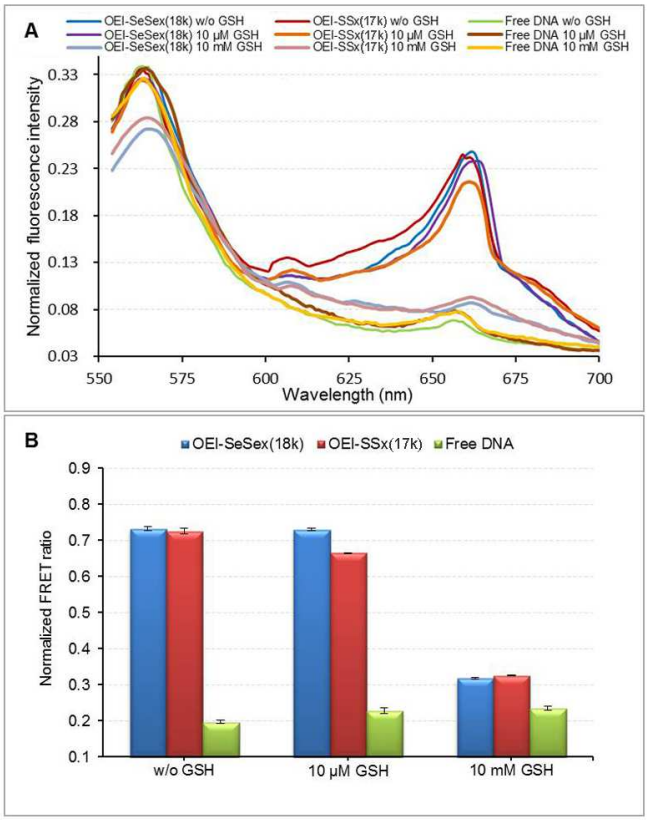

Fig.6 Representative FRET spectra of OEI-$SeSe_x$(18k) and OEI-SS_x(17k) complexes (catiomer/pDNA weight ratio, c/p = 8) acquired at 2 hours after incubation with GSH (0, 10 μM and 10 mM). Free DNA was served as control. pGL3 plasmid was dual-labeled with Cy3 and Cy5. (B) Ratio of FRET mediated Cy5 signal to Cy3 signal (I660 nm/ I565 nm), which represents complexation or disruption of the complexes after GSH treatment. Data are shown as mean ± SD (n = 3).

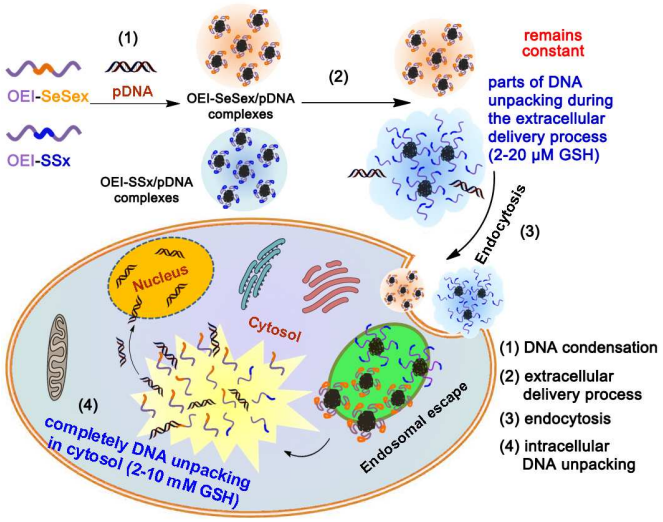

Scheme.1 Schematic representation of OEI-$SeSe_x$ and OEI-SS_x complexes for gene delivery. (1) DNA condensation (2) parts of DNA unpacking or remains constant during the extracellular delivery process (3) Endocytosis (4) completely DNA unpacking in intracellular reducing environment.

All complexes were visible as spherical aggregates with diameters around 50 nm (Fig. 5A1&B1) before GSH treatment which is smaller than that measured by DLS (120-150 nm). The discrepancy in size characterization between the two methods was predicted to arise from a shrinkage effect caused by evaporation of water in the TEM experiments.[40] After treatment with 10 μM GSH, the morphologies of OEI-$SeSe_x$(18k) complexes remained constant (Fig. 5A2), while OEI-SS_x(17k) complexes became irregular, even appeared a few large aggregates about 100 nm (Fig. 5B2). In addition, both OEI-$SeSe_x$(18k) and OEI-SS_x(17k) complexes rapidly increased to more than 300 nm after treatment with 10 mM GSH for 30 min (Fig. 5A3&B3). In conclusion, these results all confirmed that diselenide bonds are more stable than disulfide bonds, but it could be only cleaved at a tumor-relevant GSH concentration. The reductive cleavage of diselenide bonds could efficiently allow the degradation of OEI-$SeSe_x$ into low molecular weight OEI800 fragments, resulting in the rapid dissociation of OEI-$SeSe_x$ complexes.

Förster resonance energy transfer (FRET) spectrofluorometry

High extracellular stability to protect DNA against nucleases and rapid intracellular DNA unpacking is generally regarded as one important rate-limiting step for cationic non-viral vectors.[41, 42] Therefore, fluorescence resonance energy transfer (FRET) was performed here to study the DNA compaction and unpacking at gradient GSH levels (i.e. 10 μM and 10 mM GSH, mimicking the extracellular and intracellular GSH levels, respectively) following a protocol previously published.[18] DNA was dual-labeled with Cy3 and Cy5, which emits FRET signals only in the proximity (< 10 nm), and was encapsulated in OEI-SS_x(17k) and OEI-$SeSe_x$(18k) complexes. After treated with different levels of GSH, fluorescent signals (Cy3 and FRET-mediated Cy5 emissions induced by 543 nm laser) of each complexes were detected by a fluorospectrophotometer, and energy transfer was evaluated by the ratio of acceptor to donor (I_{660nm}/I_{565nm}). The normalized fluorospectra was shown in Fig. 6, which revealed that without GSH treatment, OEI-$SeSe_x$(18k)

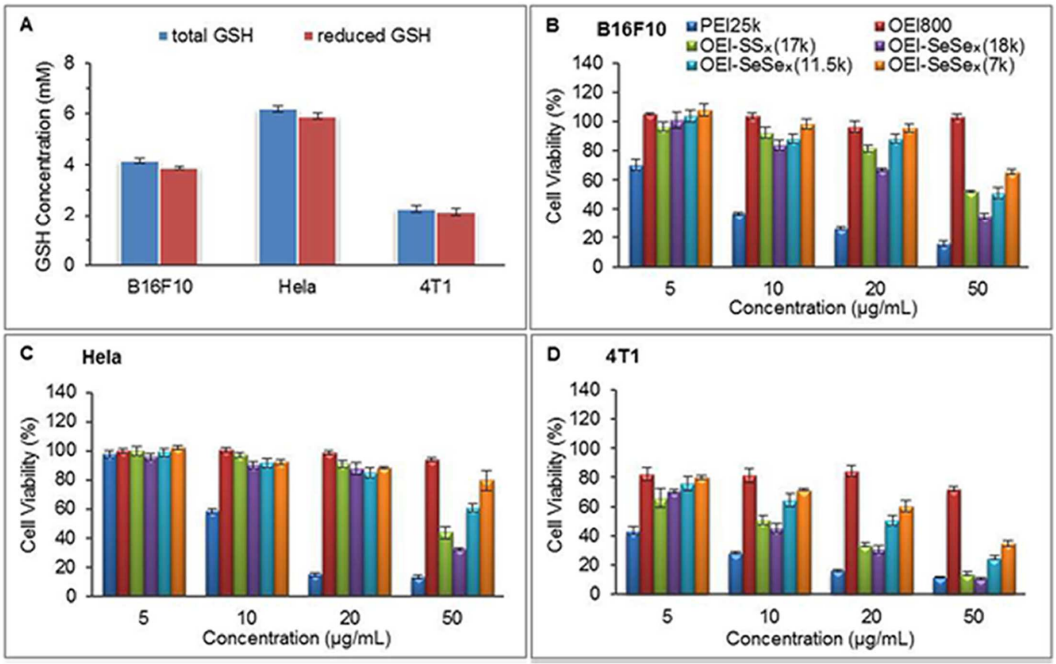

Fig.7 (A) Intracellular GSH levels of B16F10, HeLa and 4T1 Cells. Dose-dependent cytotoxicity of PEI25k, OEI800, OEI-SS_x(17k), OEI-$SeSe_x$(18k), OEI-$SeSe_x$(11.5k) and OEI-$SeSe_x$(7k) in (B) B16F10 cells, (C) HeLa cells and (D) 4T1 cells. Data are shown as mean ± SD (n = 6).

and OEI-SS_x(17k) complexes had the similar ratio of FRET (Cy5) signal to Cy3 signal about 0.74 (I_{660nm}/I_{565nm}). Difference occurred after treated with 10 μM GSH at 37 °C for 2 h. The energy transfer efficiency of OEI-SS_x(17k) complexes decreased to 0.67, while that of OEI-$SeSe_x$(18k) complexes almost remained constant. However, the difference disappeared with 10 mM GSH treatment, as little FRET signals were detected in any complexes. Besides, it is should be noted that GSH treatment had no influence on the fluorescent signals of free DNA. These results suggested that at early phase of delivery like circulation, DNA in OEI-SS_x and OEI-$SeSe_x$ complexes maintained tightly condensed, the slightly de-compaction of DNA start to occur when OEI-SS_x complexes arrive at the relatively reductive tumor site, while DNA in OEI-$SeSe_x$ complexes still maintained tightly condensed. Eventually, both of them were completely released once encountering the
elevated GSH level in cytoplasm. The difference in DNA unpacking kinetics of OEI-SS_x(17k) and OEI-$SeSe_x$(18k) can be attributed to the different reduction sensitivity of diselenide bonds and disulfide bonds. Disulfide bonds are more fragile than diselenide bonds for reductive environment. This property is not beneficial for *in vivo* gene delivery, because disulfide bonds may be cleaved during the circulation process, resulting in the payload genetics could not be delivered to their target locations.[34] In contrast, diselenide bonds not only have a high stability in 10 μM GSH conditions, but could be rapidly cleaved with 10 mM GSH treatment (Scheme 1), suggesting its great potential for *in vivo* gene delivery system's design.

Determination of intracellular GSH concentration

GSH has been well recognized as an ideal and ubiquitous internal stimulus for rapid dissociation of polyplexes inside cells to accomplish efficient intracellular gene delivery, and extensive researches have already employed this for reduction sensitive design of gene delivery vectors and gained encouraging results. However, little attention has been paid to the disparity of GSH concentrations in different tumor cells. To clarify it, as well as investigate the influence of intracellular GSH concentrations on cytotoxicity of bioreducible cationers, the intracellular GSH levels of HeLa, B16F10 and 4T1 cells were measured by a GSH and GSSG Assay protocol. The results in Fig. 7A showed that the total GSH concentration in the three tested cells were in the range of 2 mM to 7 mM, and the reduced GSH accounts for more than 90% of the total GSH. Furthermore, the intracellular GSH concentrations are different between tumor cells. For example, the total GSH concentration in HeLa cells is 6.2 ± 0.1 mM, while that for 4T1 cells is 2.3 ± 0.2 mM.

Cellular viability assessment

Clinical success of synthetic gene delivery vectors critically depends on meeting an acceptable safety profile in addition to therapeutic efficacy. In this study, *in vitro* cytotoxicity of fabricated cationers was evaluated using the B16F10, HeLa and 4T1 cells by CCK8 assay. PEI25k and OEI800 served as control. As shown in Fig. 7 (B&C&D), PEI25k was the most toxic polymer, cell viability rapidly decreased to a limiting value around 20% in all tested cells at the concentration of 20 μg/mL, attributable to its high cationic charge density.[43] In contrast, OEI800 exhibited a remarkably increased cellular viability profile even at concentration of 50 μg/mL.

The fabricated bioreducible cationers OEI-$SeSe_x$ and OEI-SS_x showed lower cytotoxicity than PEI25k. For instance, at the same concentration of 50 μg/mL, only 16% viability was found

in B16F10 cells after treatment with PEI25k, while that for

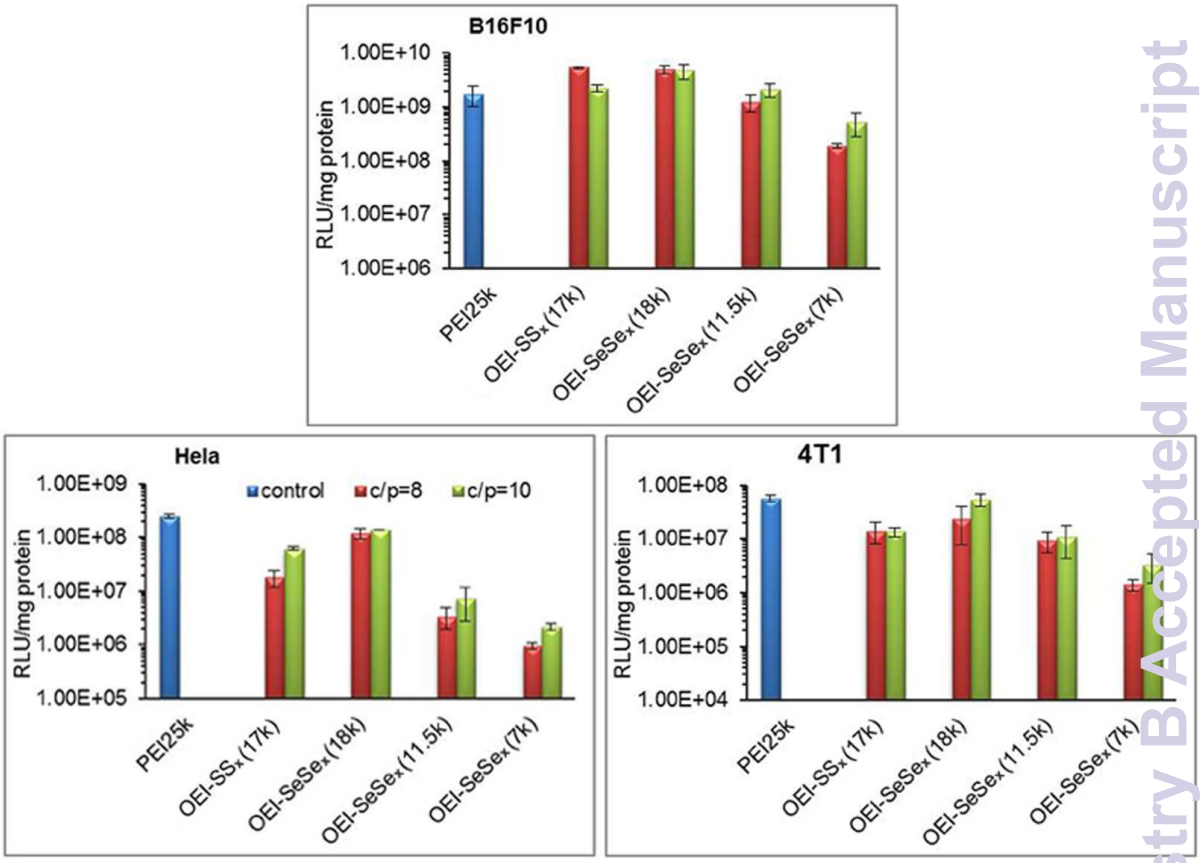

OEI-SeSe$_x$(18k), OEI-SeSe$_x$(11.5k), OEI-SeSe$_x$(7k) and OEI-

Fig.8 Luciferase transfection of the OEI-SS$_x$(17k), OEI-SeSe$_x$(18k), OEI-SeSe$_x$(11.5k) and OEI-SeSe$_x$(7k) complexes with different catiomer/pDNA ratios (8 or 10) in (A) B16F10, (B) HeLa and (C) 4T1 cells. Data are shown as mean ± SD (n = 5). PEI25k complexes (c/p = 1.3) was served as control.

SS$_x$ suggested the degradation of OEI-SeSe$_x$ and OEI-SS$_x$ via the reductive cleavage of diselenide bonds and disulfide bonds. In addition, the cytotoxicity of OEI-SeSex and OEI-SS$_x$ depends on cell type, the highest and lowest cell viability was observed in HeLa and 4T1 cells, respectively. For example, in 4T1 cells, only 30%, 50%, 60% and 33% viability were found after treatment with 20 μg/mL OEI-SeSe$_x$(18k), OEI-SeSe$_x$(11.5k), OEI-SeSe$_x$(7k) and OEI-SS$_x$(17k), respectively. While that for HeLa cells was about 88%, 85%, 88% and 91%, respectively. The highest cell viability in HeLa cells can be ascribed to its highest intracellular GSH concentration (6.2 mM), which may facilitate the rapid degradation of OEI-SeSex and OEI-SS$_x$ into less toxic and low molecular weight OEI800 fragments. As a consequence, cell viability was dramatically enhanced.

Furthermore, it is noteworthy that OEI-SeSe$_x$(18k) exhibits slightly lower cell viability than OEI-SS$_x$(17k), especially at higher concentrations. For instance, at the concentration of 50 μg/mL, the viability of OEI-SS$_x$(17k) in HeLa cells was 43%, while that for OEI-SeSe$_x$(18k) was 32%. The possible reason can be ascribed to disulfide bonds are cleaved more quickly and completely than diselenide bonds. Combined, these results indicated OEI-SeSe$_x$ showed similarly lower toxicity as OEI-SS$_x$ in comparison with PEI25k due to the reductive cleavage of diselenide bonds and disulfide bonds induced degradation of OEI-SeSe$_x$ and OEI-SS$_x$. Their cytotoxicity was cell-dependent, the highest cell viability was observed in HeLa cells, which possessed the highest intracellular GSH concentrations.

In vitro transfection of catiomer/pDNA polyplexes

The in vitro transfection efficiency of OEI-SeSe$_x$ and OEI-SS$_x$ complexes was evaluated in HeLa, B16F10 and 4T1 cells using pGL3 and pEGFP as reporter genes. PEI25k complexes at c/p ratio of 1.2 served as control. As shown in Fig. 8, the luciferase activities of OEI-SeSe$_x$ and OEI-SS$_x$ complexes depend on cell type and the highest transfection activity was observed in B16F10 cells (Fig. 8A). For example, the transfection efficiency of OEI-SeSe$_x$(18k) complexes in B16F10, HeLa and 4T1 cells was 4.9×10^9, 1.4×10^8 and 5.5×10^7 RLU/mg protein, respectively. Besides, the transfection efficiency of OEI-SeSe$_x$ increased with increasing molecular weight. At their optimum c/p ratio, OEI-SeSe$_x$(18k) and OEI-SS$_x$(17k) complexes exhibited comparable gene transfer ability to PEI25k in HeLa (Fig. 8B) and 4T1 cells (Fig. 8C). More importantly, the transfection efficiency of OEI-SeSe$_x$(18k) (4.9×10^9 RLU/mg protein) and OEI-SS$_x$(17k) (5.4×10^9 RLU/mg protein) was about 3-fold higher compared with that of PEI25k. Interestingly, the transfection efficiency of OEI-SeSe$_x$(18k) complexes was slightly higher than that of OEI-SS$_x$(17k)

complexes both in HeLa and 4T1 cells at all c/p ratios in the

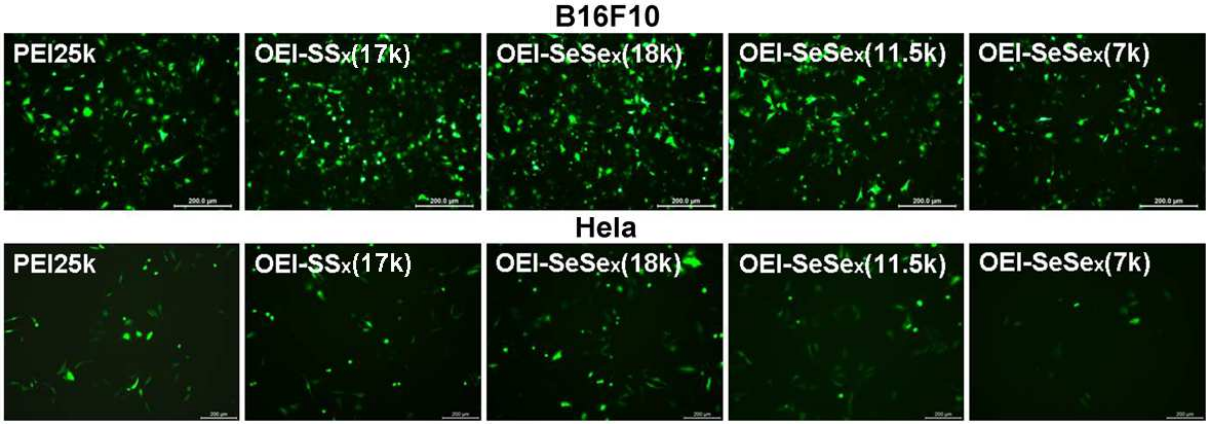

experiment. The possible reason may be ascribed to diselenide

Fig.9 pEGFP gene transfection of the OEI-SS_x(17k), OEI-$SeSe_x$(18k), OEI-$SeSe_x$(11.5k) and OEI-$SeSe_x$(7k) complexes with catiomer/pDNA ratio of 10 in B16F10 and HeLa cells. Bar = 200 nm. PEI25k (c/p = 1.3) was served as control.

bonds are stable than disulfide bonds. Following successful cellular internalization, the rapid reductive cleavage of disulfide bonds resulting in the rapid DNA unpacking. The unpacked DNA might be degraded in the harsh enzymatic environment of cytoplasm. As a consequence, the transfection efficiency was decreased.

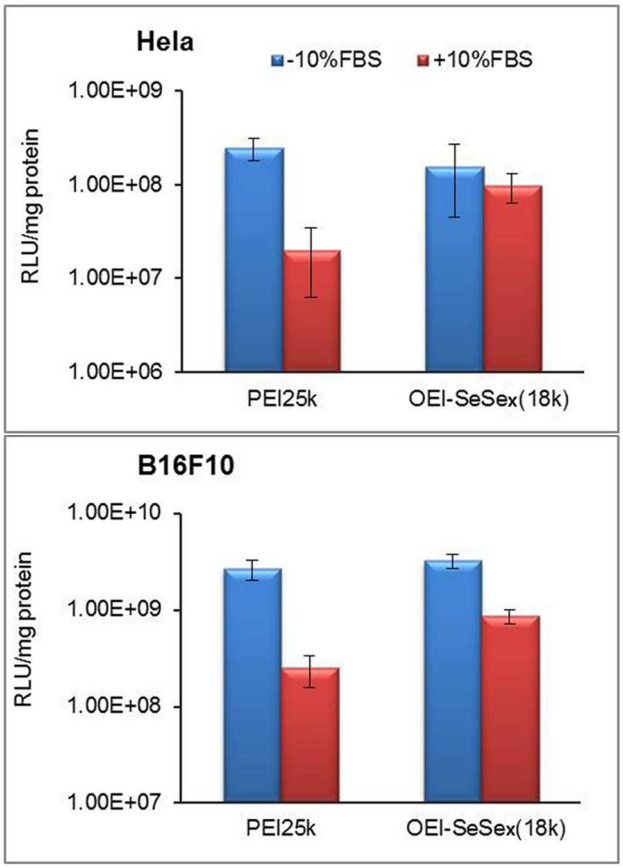

Fig.10 Effect of serum on transfection efficiency of OEI-$SeSe_x$(18k) complexes with catiomer/pDNA ratio of 10 in HeLa and B16F10 cells. PEI25k (c/p = 1.3) was served as control.

The results of qualitative studies on transfection of pEGFP with OEI-$SeSe_x$ and OEI-SS_x complexes were consistent with those for luciferase expression, which was visualized with a fluorescent microscope in B16F10 and HeLa cells. After 48 h of transfection, cells incubated with OEI-SS_x(17k) and OEI-$SeSe_x$(18k) complexes showed more bright green fluorescent pots, indicating more expression of green fluorescent protein (Fig. 9).

The significantly enhanced stability of gene vectors in serum is essential for gene therapy *in vivo*. Thus, in the present study, the effects of serum on the transfection efficiency of OEI-$SeSe_x$(18k) complexes were investigated. PEI25k (c/p = 1.3) was served as control. As shown in Fig. 10, in the presence of 10% FBS, the transfection efficiency of PEI25k complexes undergoes about 12-fold and 10-fold lower luciferase expression in Hela and B16F10 cells, respectively. However, the transfection efficiency of OEI-$SeSe_x$(18k) complexes are not apparently affected, which undergoes only about 1.6-fold and 3.7-fold lower luciferase expression in Hela and B16F10 cells, respectively. The high serum stability may be ascribed to the introduction of aliphatic chain by DSeDPA linker.[44]

Conclusions

In summary, this study systemically tested and compared the reduction sensitivity of diselenide bonds with the golden standard disulfide bonds. The experimental results demonstrated that diselenide bonds have similar reduction sensitivity as disulfide bonds, but are stable than disulfide bonds with a lower redox potential. Owing to the high stability in 10 μM GSH (mimicking the extracellular GSH levels) and rapid cleavage in 10 mM GSH (mimicking the intracellular GSH levels), diselenide bonds exhibits a great potential for *in vivo* gene delivery system's design. Cell viability assay results showed OEI-$SeSe_x$ have similar cell viability profile as OEI-SS_x, which are much lower toxic than PEI25k. More importantly, OEI-$SeSe_x$ show comparable or even outweigh

transfection efficiency as compared with OEI-SS_x and PEI25k. These results suggested that the unique properties of diselenide bonds have enabled novel and versatile designs of multifunctional bioreducible polymers for *in vivo* gene delivery.

Experimental

Materials

Selenium powder was obtained from Kelong Chemical Company (Chengdu, China). 1-ethyl-3-[3-(dimethylamino)-propyl] carbodiimide (EDC) and N-hydroxysuccinimide (NHS) were purchased from Asta Tech Pharmaceutical (Chengdu, China). 3-chloropropanoic acid, 3, 3'-disulfanediyldipropanoic acid (DSDPA), oligoethylenimine (OEI800), branched polyethylenimine 25 kDa (PEI25k), reduced glutathione and antibiotics (penicillin & streptomycin) were obtained from Sigma-Aldrich (Shanghai, China). Dulbecco's modified Eagle's medium (DMEM), fetal bovine serum (FBS) were obtained from Life Technologies Corporation (Gibco®, USA). GSH and GSSG Assay Kit were purchased from Beyotime (Nantong, China). Cell Counting Kit-8 (CCK-8) was purchased from Dojindo (Japan). Nucleic acid labeling kit Label IT® Cy5™ and nucleic acid labeling kit Label IT® Cy3™ were commercially available from Mirus Bio Corporation (USA). pEGFP-C1 (4.7 kb) and pGL3 (5.2 kb) plasmids driven by the SV40 promoter were from Promega (Madison, WI, USA), and propagated in Escherichia coli DH5α and extracted using an endotoxin-free plasmid purification kits (Qiagen, Hilden, Germany). BCA protein assay kit was purchased from Pierce (USA). Cell lysate and the luciferase reporter gene assay kit were purchased from Promega (Madison, WI). All buffers were prepared in MilliQ ultrapure water and filtered (0.22 μm) prior to use. All other chemicals were purchased from Aldrich and used as received.

Synthesis of OEI-$SeSe_x$ and OEI-SS_x

Diselenide-conjugated OEI800 (OEI-$SeSe_x$) and disulfide-conjugated OEI800 (OEI-SS_x) were obtained by cross-linking OEI800 with 3, 3'-diselanediyldipropanoic acid (DSeDPA) and 3, 3'-disulfanediyldipropanoic acid (DSDPA), respectively.

The diselenide bonds-containing linker, DSeDPA, was first synthesized according to the scheme modified from the literature.[45] In brief, selenium powder (2.37 g, 30 mmol) in 10 mL of water was mixed with $NaBH_4$ (2.27 g, 60 mmol) to obtain a colorless solution, then another quantity of selenium powder (2.37 g, 30 mmol) was added, and the mixture was heated to 105 °C for 20 minutes until it turned reddish brown. Subsequently, 3-chloropropanoic acid (6.50 g, 60 mmol) in 15 mL of water (pH, 8.0) was added to the reddish brown solution, and the reaction was maintained at room temperature for overnight under nitrogen. After another 4 hours of stirring and exposure to the atmosphere, the reaction mixture was filtered. The yellow supernatant was adjusted to pH 3-4 using 1 mol/L HCl solution and extracted with ethyl acetate. The combined organic layers were washed with water, dried with anhydrous magnesium sulfate, filtered, and recrystallized from ethyl acetate to give a product of 6.00 g (a 66% yield). ^{1}H-NMR (400 MHz, *d*6-DMSO): δ 3.05 (t, 2H), δ 2.71 (t, 2H). (Supporting Information, Figure S2).

Then, the carboxyl group at the terminal end of DSeDPA and DSDPA was activated by NHS. In brief, DSeDPA (0.52 g, 1.7 mmol) or DSDPA (0.43 g, 1.7 mmol) and NHS (0.48 g, 4.2 mmol) dissolved in 5 mL anhydrous THF were added to a three-necked flask under nitrogen with magnetic stirring. EDC (0.80 g, 4.2 mmol) dissolved in 5 mL anhydrous THF was added dropwise into the mixture at 0 °C. The reaction mixture was allowed to proceed for overnight at room temperature. After filtration, evaporation, and re-dissolution in 0.5 mL of anhydrous dimethyl sulfoxide, the active ester solution (DSeDPA-NHS, DSDPA-NHS) obtained was ready for further use.

Prior to cross-linking, OEI800 (0.50 g, 1 mmol) dissolved in water, adjusted to pH 7.4 by HCl solution, lyophilized and redissolved in 2 mL of dimethyl sulfoxide (DMSO), then mixed with various active ester solutions (DSeDPA-NHS or DSDPA-NHS) under a dry nitrogen atmosphere. In order to obtain different molecular weight OEI-$SeSe_x$, OEI800 concentration in the reaction mixture varied from 10% to 25%. The solution was stirred continuously for 2 days at 35 °C. The pure product of OEI-$SeSe_x$ and OEI-SS_x were obtained after dialysis and lyophilization. ^{1}H-NMR (400 MHz, D_2O): δ 2.36, 2.63, 2.80, 3.00, 3.10, 3.44. (Supporting Information, Figure S2).

Chemical properties of OEI-$SeSe_x$ and OEI-SS_x

Proton nuclear magnetic resonance (^{1}H NMR) spectra were recorded on a Bruker Avance II NMR spectrometer at 400 MHz using DMSO-*d*6 or D_2O as solvent, with 0.5% tetramethylsilane as internal standard.

Molecular weight and molecular weight distributions of OEI-$SeSe_x$ and OEI-SS_x were determined by Gel permeation chromatography (Waters, Milford, MA). A Waters 2690D high-pressure liquid chromatography system was equipped with ultrahydrogel 1000 and 120 columns, as well as a 2410 refractive index detector. NaCl solution 0.1 M with pH adjusted to 2.8 by HCOOH was used as eluent at a flow rate of 1.0 mL per minute. The external and column temperatures were kept at 35 °C. Pullulans of a different molecular weight (1 mg/mL) was used as the standard for the determination of calibration curve.

In order to investigate the responsiveness of the disulfide and diselenide bond to the redox milieu, OEI-$SeSe_x$ and OEI-SS_x were treated with 10 μM GSH for 4 h or 8 h, or treated with 10 mM GSH for 2 h at 37 °C, respectively. Before and after the treatment, molecular weight of the polymers was determined by GPC. PEI25k and OEI800 served as controls.

Fabrication and characterization of catiomer/pDNA complexes

Catiomer/pDNA complexes assembly

The catiomer/pDNA binary complexes was prepared by mixing catiomer and DNA solution gently at indicated catiomer/pDNA weight ratios (c/p) in HBG buffer (HEPES 20 mM, 5% (w/v) glucose, pH 7.4) and incubated at room temperature for 20 min before use.

Agarose Gel Retardation Assay

The agarose gel retardation assay was performed to assess the ability of catiomers to condense pDNA into the electrostatically stabilized polyplexes. Routinely, suspensions of various complexes (OEI-$SeSe_x$, OEI-SS_x, OEI800, PEI25k) with different catiomer/pDNA weight ratios (c/p = 0.2-0.8) were loaded onto 1% agarose gel. Electrophoresis was performed in Tris-acetate-EDTA (TAE) buffer (pH 8) running at 85 V for 40 minutes. The gel was stained with ethidium bromide (EtBr), and the resulted DNA migration patterns were

analyzed on the Molecular Imager ChemiDoc XRS+ (Bio-Rad, USA).

Particle size distribution and zeta potential

Particle size distribution and zeta potentials of fabricated catiomer/pDNA complexes were measured by Nano-ZS 90 Nanosizer (Malvern Instruments Ltd, Worcestershire, UK) according to the manufacturer's instructions. For measurements, the complexes were diluted to 1 mL with MilliQ water to a final pDNA concentration of 2 μg/mL.

Stability of the catiomer/pDNA complexes in reduction conditions

The stability of catiomer/pDNA complexes in reductive environment was evaluated by particle size and zeta potential measurement, gel retardation assay and transmission electron microscopy. The particle size and zeta potential alterations of the OEI-SS_x(17k) and OEI-$SeSe_x$(18k) complexes with a catiomer/pDNA weight ratio of 8 after treatment with 10 μM and 10 mM GSH for 30 min or 2 h were detected by Nano-ZS 90 Nanosizer. PEI25k complexes (c/p = 1.3) was served as control.

DNA release from the complexes was detected by gel retardation assay. Complexes were treated with 10 μM and 10 mM GSH for 30 min at 37 °C. Same catiomer/pDNA weight ratios (c/p) of 0.2 to 0.8 were selected for OEI-$SeSe_x$(18k) and OEI-SS_x(17k) polyplexes.

The morphology of the complexes was characterized by transmission electron microscopy. A drop of complexes (c/p = 8) suspension incubated with or without a reductive reagent was deposited on amorphous carbon-coated copper grid and detected using a JEOL JEM-100CX electron microscope (Tokyo, Japan) at an accelerating voltage of 50 kV.

Förster resonance energy transfer (FRET) spectrofluorometry

FRET spectrofluorometry was performed to investigate the DNA unpacking induced by reductive cleavage of diselenide bonds and disulfide bonds. The pGL3 plasmid was fluorescently dual-labeled with Cy3 and Cy5 using the Label IT® Kit. According to manufacturer's specifications, the average density of fluorescent dyes is one dye molecule per 380 DNA base pairs. OEI-SS_x and OEI-$SeSe_x$ polyplexes were prepared using the Cy3 and Cy5 dual-labeled pGL3. The DNA polyplexes (catiomer/pDNA weight ratio, c/p = 8) were exposed to a final concentration of 10 μM, 10 mM GSH for 2 h at 37 °C or kept untreated. Free DNA dual-labeled with Cy3 and Cy5 was served as a negative control. And the total 200 μL of DNA polyplexes solution containing 3 μg DNA was used for spectrofluorometry study. Fluorescence emission spectra from 550 to 700 nm at the step length of 5 nm and at the bandwidth of 5 nm upon excitation at 543 nm were scanned by a Spectrophotometer (F-7000 FL, Hitachi).

Cell culture

Mouse mammary carcinoma cells (4T1) and murine melanoma cells (B16F10) were obtained from Shanghai Institution for Biological Science (China), and routinely maintained at 37 °C in a humidified 5% (v/v) CO_2 atmosphere using RPMI1640, supplemented with 10% FBS and 0.1% (v/v) penicillin/streptomycin solution. Human cervical epithelial carcinoma cells (HeLa) were also obtained from Shanghai Institution for Biological Science (China), and cultured in DMEM containing 10% FBS and 0.1% (v/v) penicillin/streptomycin solution.

Determination of intracellular GSH concentration

The determination of intracellular GSH concentrations was performed following the GSH and GSSH Assay Kit protocol. In brief, 4T1, B16F10 and HeLa cells were seeded at a density of 1×10^4 cells/well (of a 96-well plate) and cultured for 1 d. The culture medium was removed and the cells were washed with PBS, pH 7.4, trypsinized, and collected in sterile tubes after a 5 min centrifugation at 1000 rpm. The supernatant was discarded, and cells were re-suspended by protein removal agent M solution. The cell suspensions were quickly freezing with liquid nitrogen and thawing with 37 °C water bath twice. The supernatant was collected for the determination of GSSG and total glutathione (GSSG + GSH) concentrations.

Cell viability assay

The cytotoxicity of OEI-$SeSe_x$ and OEI-SS_x was determined by Cell Counting Kit-8 (CCK8) assay, OEI800 and PEI25k served as control. Briefly, 4T1, B16F10 and HeLa cells were seeded into a 96-well plate at a density of 8×10^3 cells/well. Following an overnight attachment period, cells were exposed to various catiomer concentrations (5-50 μg/mL) prepared in cell culture medium. After 24 h, 10 μL CCK8 was added to each well and the plates were incubated at 37 °C for another 2 h. Absorbance was measured at a wavelength of 490 nm and a reference wavelength of 630 nm using a microplate reader (BIO-RAD 550, USA).

***In vitro* transfection**

Biological efficacy of OEI-$SeSe_x$ and OEI-SS_x was evaluated *in vitro* using pGL3 and pEGFP as reporter genes. PEI25k served as control. Transfection experiments were carried out using the HeLa, 4T1 and B16F10 cells in 96-well plates at a density of 1×10^4 cells/well. pGL3-containing polyplexes with a catiomer/pDNA weight ratio of 8 or 10 were fabricated in serum-free or 10% serum-containing culture medium and added to each well (0.2 μg DNA/well). Following a 4 h incubation at 37 °C in a humidified atmosphere with 5% CO_2, the medium was replaced with fresh culture medium containing 10% FBS, and cells were incubated for additional 24 h. For luciferase assay, the medium was removed, and the cells were washed with PBS, then lysed using reporter lysis buffer. The luciferase activity was measured with chemiluminometer (BIO-RAD 550, USA) according to manufactures protocol. The luciferase activity was normalized to the amount of total protein in the sample, which was determined using a BCA protein assay kit (Pierce, USA). For qualitative evaluation of pEGFP expression, pEGFP-containing complexes were separately transferred to B16F10 and HeLa cells in terms of the aforementioned method. At 44 h post-transfection, pEGFP-expresssing cells were visualized under a fluorescence microscope (Leica, Germany).

Acknowledgments

This study was supported by National Basic Research Program of China (National 973 program, No. 2011CB606206), National Science Foundation of China (NSFC, No. 51133004, 81361140343, 31271020), Science Foundation for the Excellent Youth Scholars of Sichuan University (2011SCU04A14) and

Research Fund for the Doctoral Program of Higher Education of China (Grant No. 20100181120075)

Notes and references

National Engineering Research Center for Biomaterials, Sichuan University, Chengdu 610064, China. E-mail: cxj520118@aliyun.com; zwgu@scu.eud.cn; Fax: +86 28 85410653; Tel: +86 28 85412923

† Electronic Supplementary Information (ESI) available: See DOI: 10.1039/b000000x/

1. M. Candolfi, W. Xiong, K. Yagiz, C. Liu, A. K. M. G. Muhammad, M. Puntel, D. Foulad, A. Zadmehr, G. E. Ahlzadeh, K. M. Kroeger, M. Tesarfreund, S. Lee, W. Debinski, D. Sareen, C. N. Svendsen, R. Rodriguez, P. R. Lowenstein and M. G. Castro, *Proc. Natl. Acad. Sci. U. S. A.,* 2010, **107**, 20021-20026.
2. L. C. Yin, Z. Y. Song, K. H. Kim, N. Zheng, N. P. Gabrielson and J. J. Cheng, *Adv. Mater.*, 2013, **25**, 3063-3070.
3. C. M. Curtin, G. M. Cunniffe, F. G. Lyons, K. Bessho, G. R. Dickson, G. P. Duffy and F. J. O'Brien, *Adv. Mater.*, 2012, **24**, 749-754.
4. P. S. Ghosh, C.-K. Kim, G. Han, N. S. Forbes and V. M. Rotello, *ACS Nano*, 2008, **2**, 2213-2218.
5. Z. H. Liu, Z. Y. Zhang, C. R. Zhou and Y. P. Jiao, *Prog. Polym. Sci.*, 2010, **35**, 1144-1162.
6. X. J. Cai, C. Y. Dong, H. Q. Dong, G. M. Wang, G. M. Pauletti, X. J. Pan, H. Y. Wen, I. Mehl, Y. Y. Li and D. L. Shi, *Biomacromolecules*, 2012, **13**, 1024-1034.
7. H. Uchida, K. Miyata, M. Oba, T. Ishii, T. Suma, K. Itaka, N. Nishiyama and K. Kataoka, *J. Am. Chem. Soc.*, 2011, **133**, 15524-15532.
8. H. Y. Wang, J. X. Chen, Y. X. Sun, J. Z. Deng, C. Li, X. Z. Zhang and R. X. Zhuo, *J. Controlled Release*, 2011, **155**, 26-33.
9. X. J. Cai, H. Q. Dong, J. P. Ma, H. Y. Zhu, W. Wu, M. Chu, Y. Y. Li and D. L. Shi, *J. Mater. Chem. B*, 2013, **1**, 1712-1721.
10. M.-H. Kim, H.-K. Na, Y.-K. Kim, S.-R. Ryoo, H. S. Cho, K. E. Lee, H. Jeon, R. Ryoo and D.-H. Min, *ACS Nano*, 2011, **5**, 3568-3576.
11. R. L. Zhao, B. Sun, T. Y. Liu, Y. Liu, S. M. Zhou, A. J. Zuo and D. C. Liang, *Int. J. Pharm.*, 2011, **413**, 254-259.
12. B. B. Sun, K. K. Tran and H. Shen, *Biomaterials*, 2009, **30**, 6386-6393.
13. K. Luo, C. X. Li, G. Wang, Y. Nie, B. He, Y. Wu and Z. W. Gu, *J. Controlled Release*, 2011, **155**, 77-87.
14. T. G. Park, J. H. Jeong and S. W. Kim, *Adv. Drug Delivery Rev.*, 2006, **58**, 467-486.
15. T.-i. Kim, M. Lee and S. W. Kim, *Biomaterials*, 2010, 31, 1798-1804.
16. T.-i. Kim, M. Ou, M. Lee and S. W. Kim, *Biomaterials*, 2009, **30**, 658-664.
17. Y. Y. He, G. Cheng, L. Xie, Y. Nie, B. He and Z. W. Gu, *Biomaterials*, 2013, **34**, 1235-1245.
18. P. S. Xu, G. K. Quick and Y. Yeo, *Biomaterials*, 2009, **30**, 5834-5843.
19. Y. H. Kim, J. H. Park, M. Lee, Y.-H. Kim, T. G. Park and S. W. Kim, *J. Controlled Release*, 2005, **103**, 209-219.
20. J. Dai, S. Y. Zou, Y. Y. Pei, D. Cheng, H. Ai and X. T. Shuai, *Biomaterials*, 2011, **32**, 1694-1705.
21. Y. T. Wen, S. R. Pan, X. Luo, X. Zhang, W. Zhang and M. Feng, *Bioconjugate Chem.*, 2009, **20**, 322-332.
22. I.-K. Park, K. Singha, R. B. Arote, Y.-J. Choi, W. J. Kim and C.-S. Cho, *Macromol. Rapid Commun.*, 2010, **31**, 1122-1133.
23. W. W. Gao, J. M. Chan and O. C. Farokhzad, *Mol. Pharm.*, 2010, **7**, 1913-1920.
24. J. Zhang, Z. F. Yuan, Y. Wang, W. H. Chen, G. F. Luo, S. X. Cheng, R. X. Zhuo and X. Z. Zhang, *J. Am. Chem. Soc.*, 2013, **135**, 5068-5073.
25. S. X. Huang, K. Shao, Y. Y. Kuang, Y. Liu, J. F. Li, S. An, Y. B. Guo, H. J. Ma, X. He and C. Jiang, *Biomaterials*, 2013, **34**, 5294-5302.
26. T.-i. Kim and S. W. Kim, *React. Funct.Polym.,* 2011, **71**, 344-349.
27. R. Cheng, F. Feng, F. H. Meng, C. Deng, J. Feijen and Z. Y. Zhong, *J. Controlled Release*, 2011, **152**, 2-12.
28. W. Y. Li, P. Zhang, K. Zheng, Q. L. Hu and Y. X. Wang, *J. Mater. Chem. B*, 2013, **1**, 6418-6426.
29. F. H. Meng, W. E. Hennink and Z. Y. Zhong, *Biomaterials*, 2009, **30**, 2180-2198.
30. L. V. Christensen, C.-W. Chang, W. J. Kim, S. W. Kim, Z. Y. Zhong, C. Lin, J. F. J. Engbersen and J. Feijen, *Bioconjugate Chem.*, 2006, **17**, 1233-1240.
31. Y. X. Wang, P. Chen and J. C. Shen, *Biomaterials*, 2006, **27**, 5292-5298.
32. J. Liu, X. L. Jiang, L. Xu, X. M. Wang, W. E. Hennink and R. X. Zhuo, *Bioconjugate Chem.*, 2010, **21**, 1827-1835.
33. N. Ma, Y. Li, H. P. Xu, Z. Q. Wang and X. Zhang, *J. Am. Chem. Soc.*, 2009, **132**, 442-443.
34. G. Cheng, Y. Y. He, L. Xie, Y. Nie, B. He, Z. R. Zhang and Z. W. Gu, *Int. J. Nanomed.*, 2012, **7**, 3991-4006.
35. H. J. Yu, V. Russ and E. Wagner, *AAPS J.*, 2009, **11**, 445-455.
36. T. Wang, J. R. Upponi and V. P. Torchilin, *Int. J. Pharm.*, 2012, **427**, 3-20.
37. R. L. Sheng, T. Luo, Y. D. Zhu, H. Li, J. J. Sun, S. D. Chen, W. Y. Sun and A. Cao, *Biomaterials*, 2011, **32**, 3507-3519.
38. Y. M. Liu and T. M. Reineke, *J. Am. Chem. Soc.*, 2005, **127**, 3004-3015.
39. Q. Peng, Z. L. Zhong, and R. X. Zhuo, *Bioconjugate Chem.*, 2008, **19**, 499–506.
40. X. J. Cai, H. Q. Dong, W. J. Xia, H. Y. Wen, X. Q. Li, J. H. Yu, Y. Y. Li and D. L. Shi, *J. Mater. Chem.*, 2011, **21**, 14639-14645.
41. C. L. Grigsby and K. W. Leong, *J. R. Soc. Interface*, 2010, **7**, S67-S82.
42. M. Thibault, S. Nimesh, M. Lavertu and M. D. Buschmann, *Mol. Ther.*, 2010, **18**, 1787-1795.
43. D. Fischer, T. Bieber, Y. Li, H.-P. Elsässer and T. Kissel, *Pharm. Res.*, 1999, **16**, 1273-1279.
44. V. Russ, H. Elfberg, C. Thoma, J. Kloeckner, M. Ogris, E. Wagner, *Gene Ther.* 2008, **15**, 18-29.
45. T. Koch, E. Suenson, U. Henriksen and O. Buchardt, *Bioconjugate Chem.*, 1990, **1**, 296-304.

Table of Contents:

Diselenide bonds as a new reduction-sensitive linkage is proposed for developing bioreducible polycation for non-viral gene delivery system. Compared with the golden standard disulfide bonds, diselenide bonds can also timely release DNA inside the tumor cells, while remain constant outside the cells, implying its higher stability during the circulation process and great potential for *in vivo* gene delivery system's design.